

Fatigue in Breakwater Concrete Armour Units

Burcharth, Hans F.

Published in:

Proceedings of the 19th International Conference on Coastal Engineering : ICCE '84

Publication date:
1985

Document Version
Publisher's PDF, also known as Version of record

[Link to publication from Aalborg University](#)

Citation for published version (APA):

Burcharth, H. F. (1985). Fatigue in Breakwater Concrete Armour Units. In B. L. Edge (Ed.), *Proceedings of the 19th International Conference on Coastal Engineering : ICCE '84: Houston, Texas, September 3-7 1984* (pp. 2592-2607). American Society of Civil Engineers.

General rights

Copyright and moral rights for the publications made accessible in the public portal are retained by the authors and/or other copyright owners and it is a condition of accessing publications that users recognise and abide by the legal requirements associated with these rights.

- Users may download and print one copy of any publication from the public portal for the purpose of private study or research.
- You may not further distribute the material or use it for any profit-making activity or commercial gain
- You may freely distribute the URL identifying the publication in the public portal -

Take down policy

If you believe that this document breaches copyright please contact us at vbn@aub.aau.dk providing details, and we will remove access to the work immediately and investigate your claim.

CHAPTER ONE HUNDRED SEVENTY FOUR

FATIGUE IN BREAKWATER CONCRETE ARMOUR UNITS

Hans F. Burcharth *

ABSTRACT

The reliability of rubble mound breakwaters depends on the hydraulic stability and the mechanical strength of the armour units. The paper deals with the important aspect of fatigue related to the strength of concrete armour units.

Results showing significant fatigue from impact tests with Dolosse made of unreinforced and steel fibre reinforced flyash concrete are presented. Moreover universal graphs for fatigue in armour units made of conventional unreinforced concrete exposed to impact load and pulsating load are presented. The effect of fibre reinforcement and the implementation of fatigue in a stochastic design process are discussed.

INTRODUCTION

Many of the recent failures of large rubble mound breakwaters are due to unexpected fracture of the concrete armour units. Traditionally the design process is based on hydraulic model tests and the design criterion chosen with consideration only to the hydraulic stability. Although progress has been made during the last years there exists no consistent armour layer design method in which both the hydraulic and the mechanical stability are considered. A discussion on the state of the art of this problem is given in Burcharth, 1983 (ref. 1 and 2).

The different types of loads on armour units and their origin are listed in Fig. 1.

TYPES OF LOADS		ORIGIN OF LOADS
STATIC		Weight of units
		Prestressing due to: Settlement of underlayers Wedge effect and arching due to movements under dynamic loads
ABRASION		Suspended material
DYNAMIC	Impact	Rocking/rolling of units Missiles of broken units Placing during construction
	Pulsating	Earthquake Gradually varying wave force
THERMAL		Stresses due to temperature differences during hardening process Freeze-thaw
CHEMICAL		Corrosion of reinforcement Sulfate reactions etc.

Fig. 1. Types of loads on armour units.

* Professor of Marine Civil Engineering, University of Aalborg, Denmark.

This paper deals with fatigue due to repeated dynamic loads from the waves. Fatigue is the reduction in material strength by increasing number of load cycles.

FATIGUE

The waves will cause *pulsating* (gradually varying) flow forces and also *impact* forces when the units are rocking. The number of cycles of wave loadings will be in the order of 200 million during a 50 years' period in the North Atlantic period. Since 1903 it has been known that concrete shows significant fatigue. Considering the high stress level in the large slender types of units such as Dolosse and Tetrapods it is important to evaluate the fatigue effect on the stability.

Fig. 2 shows the results from uniaxial fatigue tests with small specimens by Tepfers et al., 1979 (ref. 3 and 4), Fagerlund et al., 1979 (ref. 5), Zielinski et al., 1981 (ref. 6). The size of the specimens were 150 mm cubes, 100 mm and 74 mm diameter cylinders.

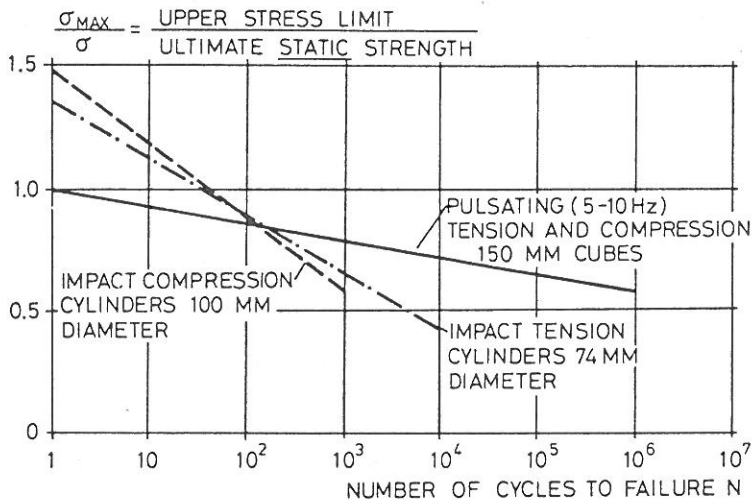


Fig. 2. Fatigue. Uniaxial impact and pulsating loading of small specimens (Tepfers et al. 1979, Fagerlund et al. 1979, Zielinski et al. 1981).

The results of the static test shown in Fig. 2 compare very well to the results by Tait et al., 1980 (ref. 7) for 25 kg model Dolosse of 300 mm height exposed to a pulsating load which created mainly uniaxial tensile stresses in the critical section, see Fig. 3.

Impact tests by M.G.A. Silva, 1983 (ref. 8) with full scale cubes in the range 1 ton to 27 tonnes also revealed significant fatigue as shown in Fig. 4. In the tests one cube impacted side to side a resting cube of the same size.

From the above mentioned tests it is seen that impact loads create the most drastic reduction in strength. Regarding the application in practical breakwater design of the tests presented in Fig. 2 and 3 it might be argued that the size of the specimens could be too small to re-

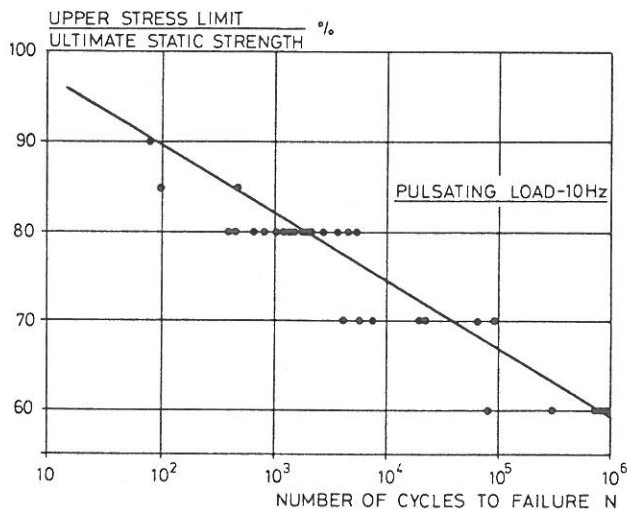


Fig. 3. Fatigue. Uniaxial pulsating tension loading of model Dolosse of 300 mm height (Tait et al. 1980).

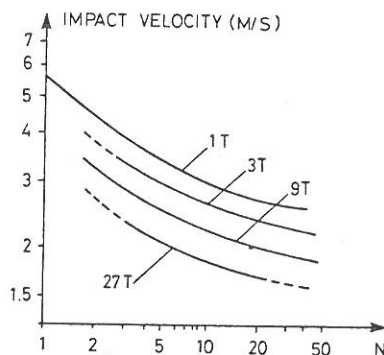


Fig. 4. Fatigue. Impact tests with full scale cubes (M. G. A. Silva 1983).

present the properties of prototype concrete. Also the stresses are uniaxial whereas in prototype the stresses in critical sections are often flexural stresses. To evaluate these questions series of impact fatigue flexural stress tests with 200 kg Dolosse were performed at the University of Aalborg from 1981 to 1983. Both unreinforced and steel fibre reinforced concrete were tested.

FATIGUE TEST SET UP AND TEST PROGRAMME

The test set up is shown in Fig. 5.

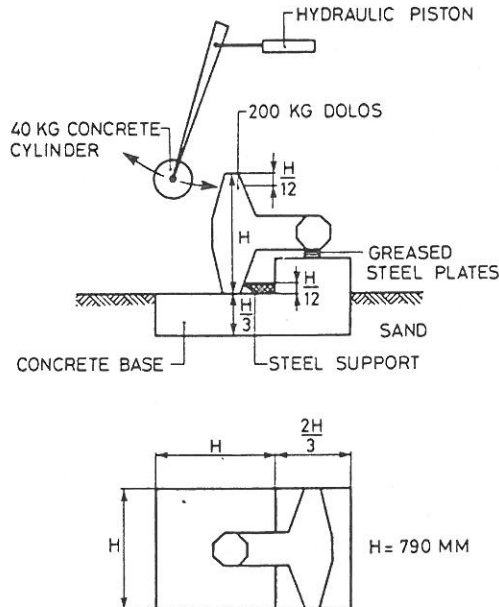


Fig. 5. Set up of Dolosse impact fatigue tests.

The support of the Dolosse compares to the set up used in prototype dynamic testing of Dolosse proposed by Burcharth 1980 and 1981 (ref. 9 and 10) and since widely used by other researchers. The set up is designed to generate mainly flexural stresses in the critical sections of the stem and the leg near the stem/leg corner. The pendulum was automatically operated by a hydraulic piston which could be set to any draw back distance from which the pendulum was released, thus reaching a specific impact speed. The number of impacts were recorded automatically. The operating speed was approximately one impact per 2 sec, somewhat dependent on the draw back distance.

Apart from disintegration also the first sign of crack and a specific width of the crack were taken as failure modes to be registered. This necessitated careful visual observation of the Dolosse throughout the tests.

To prevent material scale effects the size of the Dolosse was chosen such that concrete with normal size of aggregates could be used. This resulted in a Dolosse height of 790 mm, a stem diameter of 261 mm giving a waist ratio of 0.33 and a mass of approximately 200 kg. The diagonal of the stem leg corner fillets was 48 mm.

A total of 45 Dolosse were tested included some pilot tests. Two types of concrete, unreinforced flyash concrete and steel fibre reinforced flyash concrete, were tested. The specifications and the material properties are listed in Table 1.

Table 1. Specifications of concretes.

	Unreinforced units	Steelfibre reinforced units
Cement content kg/m ³	380 portland	435 portland flyash cement
Flyash kg/m ³	125	
Sand kg/m ³	525	788
4-8 mm pebbles kg/m ³	80	none
8-16 mm pebbles kg/m ³	1095	416
16-32 mm stones kg/m ³	none	416
Water cement ratio	0.45	0.40
Additives	app. 4% air in Dolosse	3.3 kg plastisizer BV 40 app. 6% air in Dolosse
Reinforcement kg/m ³	none	160, Wirex steel fibre 45 × 1 mm plain round (2% by volume)
Mean static compressive strength 100 × 200 mm cyl. $\bar{\sigma}_c$ N/mm ²	44.4	27.0 *)
Mean static tensile strength 100 × 200 mm cyl. splitting test $\bar{\sigma}_{T \text{ split}}$ N/mm ²	3.65	3.47 *)
Mean modulus of elasticity determined by ultrasound measurement \bar{E} N/mm ²	4.4 × 10 ⁴	
Mean mass density of concrete in Dolosse $\bar{\rho}$ kg/m ³	2330	2300

*) Absolute values not fully representative for the Dolosse concrete strength due to boundary effect of the small cylinders on the concrete containing large fibres and coarse aggregates. This resulted in app. 4% higher air content and accordingly lower strength properties for the cylinder specimens. On this base the strength of the concrete in the Dolosse is estimated to $\bar{\sigma}_c = 30 \text{ N/m}^2$ and $\bar{\sigma}_T = 3.85 \text{ N/mm}^2$.

A fairly high fibre content of 160 kg per m³ of concrete or 2% by volume was used to make sure that it was well above the limit where fibre has no effect. According to full scale tests with 30 t Dolosse (static test and drop test) conducted by the author a steel fibre content below 70 kg/m³ has only negligible effect on the strength.

Pilot's tests with beams reinforced with various types of steel fibres showed that a fibre length of app. 45 mm ensured a good toughness. A somewhat smaller diameter of the fibre than the applied 1 mm would probably have been more effective in terms of toughness per kilo of steel.

Although the amount of fibres was high no problems with mixing of the fibres were observed and the distribution of the fibres in the concrete Dolosse was good. However, the air content came out higher than expected and the strengths lower.

The age of all units when tested were approximately one year.

THEORETICAL CONSIDERATIONS ON THE PROCESSING AND REPRESENTATION OF THE TEST RESULTS

In fatigue tests each specimen is exposed to repeated load representing a specific stress range, $\Delta\sigma$.

Neglecting the influence of the rate of strain on stress and the variation of Poisson's ration Burcharth 1981 (ref. 10) derived formulae for the maximum tensile stress in a Dolosse exposed to impact load in a drop test and a pendulum test. Taking the waist ratio as a constant (0.33 in the present tests) the two formulae are given by

$$\frac{\sigma_T}{mghH^{1/3}} \sim \left(\frac{E}{\rho gh} \right)^{0.5} \quad (1)$$

where \sim means proportional to

σ_T	the max tensile stress
m	the pendulum mass (or the Dolos mass in the drop test)
h	the pendulum fall height (or the Dolos centre of gravity fall height in the drop test)
H	the Dolos height
g	the gravitational constant
E	the dynamic or static modulus of elasticity
ρ	the mass density of pendulum and Dolos

In this it is assumed that for each type of concrete there is a constant ratio between the dynamic and the static modulus of elasticity. Thus the variation of this ratio with the stress level and the amount of internal fracture is neglected.

Eq. (1) is based on the assumption that the duration of the impact Δt can be taken as the time which elapses for a longitudinal shock wave to travel from the point of impact to a free edge of the concrete and back again, i.e. Δt is proportional to a characteristic length, H . However, actual recordings of the impact time in the present tests showed bigger values of Δt . A reanalysis based on the assumption of Δt being half of the natural period for the first mode of vibration of the Dolos when hit revealed good agreement between measured and calculated values of Δt . Fortunately this finding do not change eq. (1) as also the vibration model involves proportionality between Δt and a characteristic length.

Since the stresses range from approximately zero for each impact in the tests, the maximum stresses also represent the stress range. Thus in eq. (1) $\sigma_T = \Delta\sigma_T$.

The present fatigue test results are presented in diagrams where the ratio of the ultimate dynamic tensile stress range for N Impacts, $\Delta\sigma_N$ to the same quantity for one impact, $\Delta\sigma_{N=1}$

is plotted against the number of impacts at failure, N . Since the stresses were not directly recorded in the tests the ratio $\Delta\sigma_N/\Delta\sigma_{N=1}$ was determined from the impact speed (or fall height) of the pendulum as follows:

For a system with constant values of g , m and H eq (1) reduces to

$$\Delta\sigma_T \sim \left(\frac{Eh}{\rho}\right)^{0.5} \quad (2)$$

Moreover since ρ and E were approximately constants for each type of concrete we get

$$\Delta\sigma_T \sim h^{0.5} = \frac{v}{(2g)^{0.5}} \quad (3)$$

where v is the pendulum impact velocity.

Since the material properties of concrete produced to identical specifications vary, corrections for this variation should be implemented in the results. For this reason 6 cylinders (100 x 200 mm) were cast from the batch of each Dolos. 4 or 3 cylinders were used to determine the splitting tensile strength, σ_{Tsplit} and 3 or 4 cylinders were used to determine the compressive strength, σ_C . As testing of the cylinders and the corresponding Dolos took place at the same time it is assumed that the mean values $\bar{\sigma}_{Tsplit}$ and $\bar{\sigma}_C$ characterize the actual strength properties of the Dolos.

In the impact fatigue tests the relevant strength property is the dynamic tensile strength σ_{Tdyn} and not σ_{Tsplit} which, due to the splitting test procedure, is a static tensile strength property. However, in what follows the reasonable assumption of proportionality between the two tensile strengths is used for each specific type of concrete.

To make it possible to compare fatigue in Dolosse of different concrete strength, corrections for the variations as found from the cylinder splitting test can be made by means of eq. (3). Thus a measure of a characteristic stress range for a tested Dolos is

$$\Delta\sigma_a = k \frac{h_a^{0.5}}{\sigma_{Tsplit,a}} \quad (4)$$

where k is an unknown constant and indices a corresponds to a specific Dolos.

From this we obtain

$$\frac{\Delta\sigma_{N,a}}{\Delta\sigma_{N=1,b}} = \frac{h_{N,a}^{0.5} / \sigma_{Tsplit,a}}{h_{N=1,b}^{0.5} / \sigma_{Tsplit,b}} \quad (5)$$

where indices b refers to a specific Dolos.

It should be noted that the use of eq. (4) in the present tests is somewhat invalidated by the uncertainty on estimating σ_{Tsplit} from relatively small cylinders, cf. the footnote in Table 1. However, the test result presented by the graphs in Figs. 8 - 10 are based on eq. (5) which is not significantly biased because σ_{Tsplit} appears both in the nominator and the denominator.

$h_{N=1}$ in eq. (5) could not be found directly from a test because it is impossible to determine the pendulum speed which in just one impact on an untested unit causes exactly the ulti-

mate stress where the first crack appears. Therefore $\Delta\sigma_{N=1}$ was determined by extrapolation to $N = 1$ of the fatigue test results in a log-linear representation, see Figs. 6 and 7.

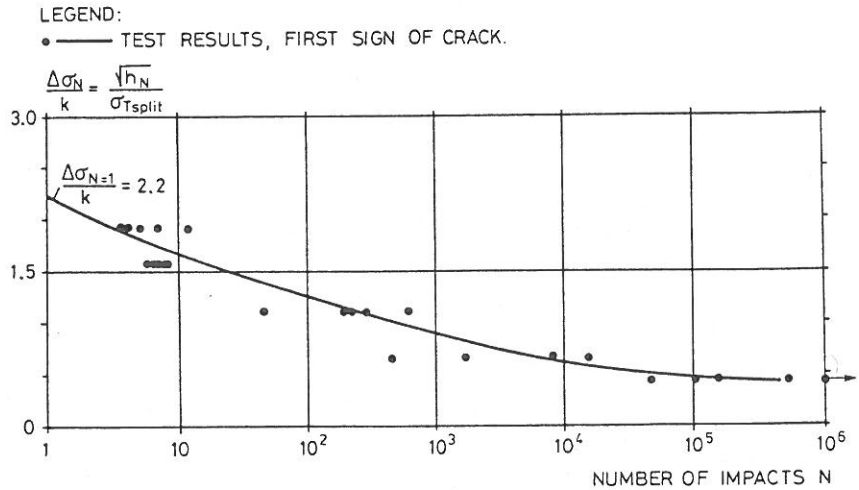


Fig. 6. Determination of $\Delta\sigma_{N=1}$ for unreinforced flyash concrete Dolosse. Flexural stress.

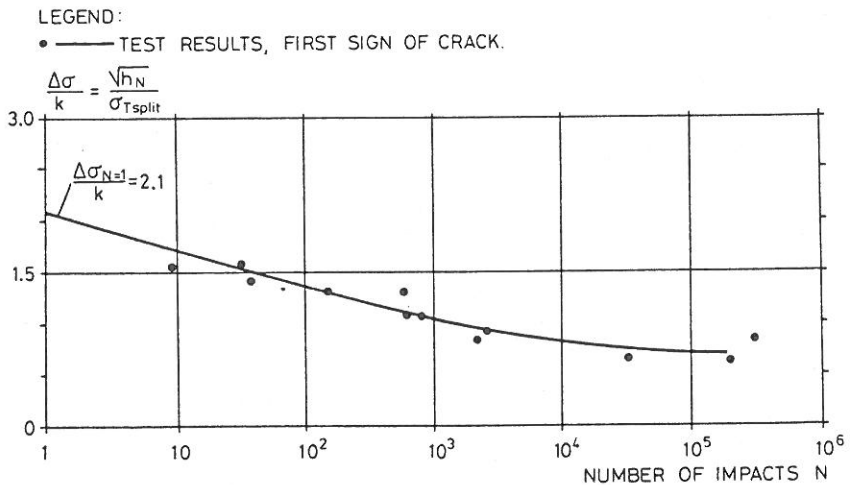


Fig. 7. Determination of $\Delta\sigma_{N=1}$ for steel fibre reinforced concrete Dolosse. Flexural stress.

TEST RESULTS

Fig. 8 shows the result of the fatigue tests with unreinforced Dolosse.

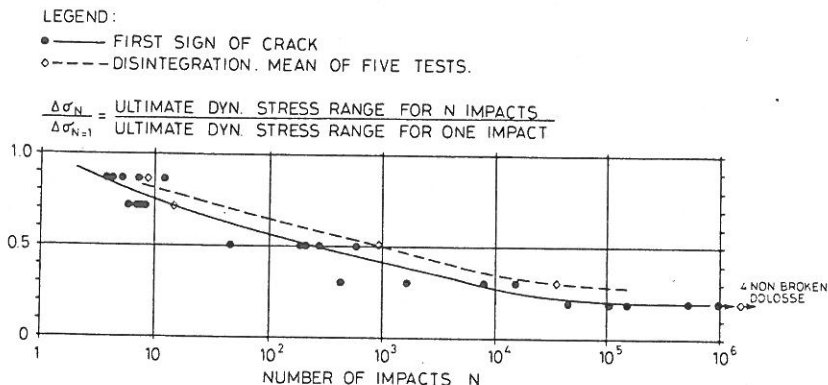


Fig. 8. Fatigue. Impact loaded Dolosse of unreinforced fly ash concrete. Flexural stress.

The ordinate represents the ratio between two dynamic stresses, namely the ultimate dynamic stress range for N impacts to the same quantity for one impact, $N = 1$. Very often in such Wöhler diagrams the denominator is the static strength (cf. Fig. 2), but the presentation in Fig. 8 demonstrates the fatigue effect more clearly.

The full line corresponds to the first sign of crack, thus representing the design graph. The dotted line shows the state of disintegration. No sign of damage or indentation of the impacted Dolos-surfaces was seen in the test series with unreinforced concrete.

The results for the fibre reinforced units are shown in Fig. 9.

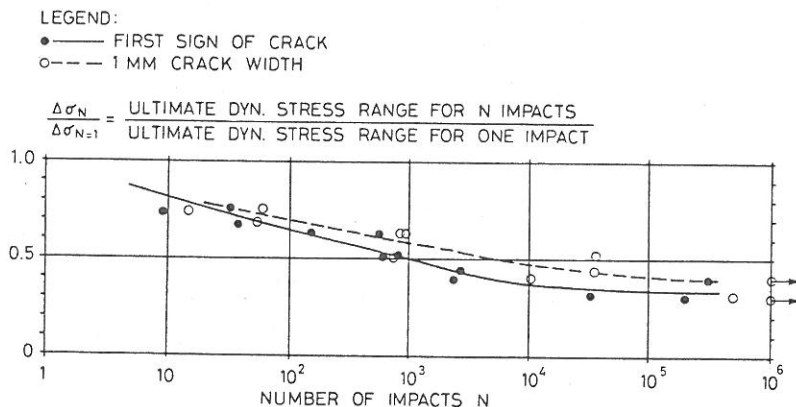


Fig. 9. Fatigue. Impact loaded Dolosse of steel fibre reinforced fly ash concrete. Flexural stress.

The full line corresponds to the first sign of crack and the dotted line to a crack width of 1 mm. For design purpose, the full line should be used since a crack width of 1 mm implies fast corrosion of the tiny steel fibres. If non-corrosive fibres are used cracks of some size might be acceptable. By large numbers of impacts an indentation was clearly seen on the impacted surface — quite contrary to the case of unreinforced concrete.

A comparison of the fatigue properties of the two types of concrete is presented in Fig. 10.

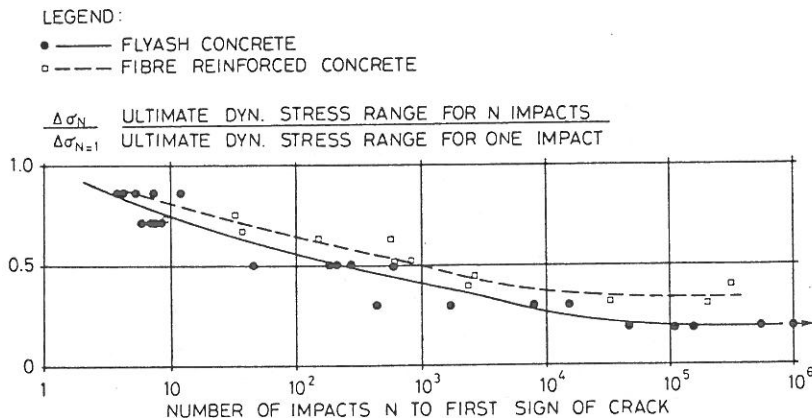


Fig. 10. Comparison of fatigue in impact loaded Dolosse of unreinforced and steel fibre reinforced flyash concrete. Flexural stress.

It is seen that the fatigue effect is smaller in the fibre reinforced units as it stabilizes at a stress range twice as big as for the unreinforced units for $N \geq 10^5$. This better performance is properly partly due to the development of a more soft impact surface, cf. the observed indentation.

Fig. 11 shows a comparison of the ultimate impact energy at the first sign of a crack. The impact energy, taken as the maximum kinetic energy of the pendulum, is dimensionless by dividing by gMH , where g is the gravitational constant, M the mass of the Dolos and H the height of the Dolos.

It is seen that, the fatigue life of the steel fibre reinforced concrete is the best of the two except for small number of impacts. However, the difference is fairly small and probably much smaller than most people expect since it is often said in the literature that fibres increase the energy absorbtions at failure many times, compared to plain concrete.

For example in ref. (11) a factor of "at least ten times" is related to a steel fibre content of 100 kg/m^3 .

The reason for this discrepancy is the fact that most testing of fibre reinforced concrete reported in the literature is done with rather slender specimens, such as beams, where large deflection creates only very small cracks, contrary to what is the case with stiff bodies like Dolosse and Tetrapods. Another important reason is that in the case of armour units failure must be defined as the appearance of a crack, while in the concrete literature failure of tested specimens is usually taken as the state of complete disintegration or some high level of deformation.

LEGEND:

○ — FLYASH CONCRETE $\bar{\sigma}_t = 3.65 \text{ N/MM}^2$ ● — FIBRE REINFORCED CONCRETE. $\bar{\sigma}_t = 3.85 \text{ N/MM}^2$. STEEL FIBRE $45 \times 1 \text{ MM} - 160 \text{ KG/M}^3$

m AND v MASS AND IMPACT VELOCITY OF PENDULUM.

M AND H MASS AND HEIGHT OF DOLOS.

g GRAVITATIONAL CONSTANT.

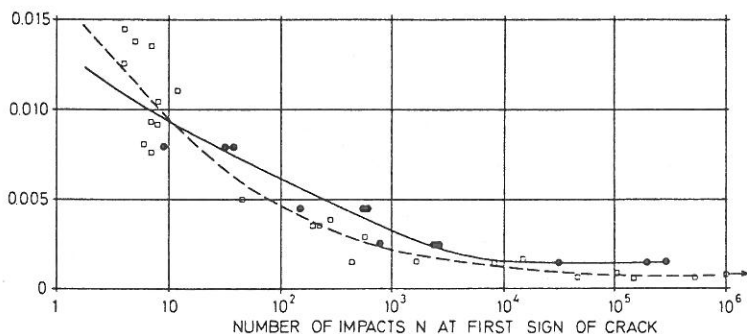
$$\frac{\frac{1}{2}mv^2}{MgH} = \text{DIMENSIONLESS ULTIMATE IMPACT ENERGY (PER IMPACT)}$$


Fig. 11. Fatigue. Comparison of ultimate impact energy for impact loaded Dolosse of unreinforced and steel fibre reinforced flyash concrete. Flexural stress.

The effect of steel fibres on the fatigue life and on the impact strength of slender armour units seems to be small and is certainly much smaller than the effect of similar quantities of steel in a conventional bar reinforcement, cf. also discussion of reinforcement in ref. (1).

In Fig. 12 the results of the present flexural impact tests with unreinforced concrete (Fig. 8) are shown together with the results of the uniaxial impact tests with small specimens (Fig. 2).

LEGEND:

— FLEXURAL, 200 KG DOLOSSE - FIRST SIGN OF CRACK

--- FLEXURAL, 200 KG DOLOSSE - DISINTEGRATION.

— UNIAXIAL TENSION, 74 MM CYLINDER

..... UNIAXIAL COMPRESSION, 100 MM CYLINDER

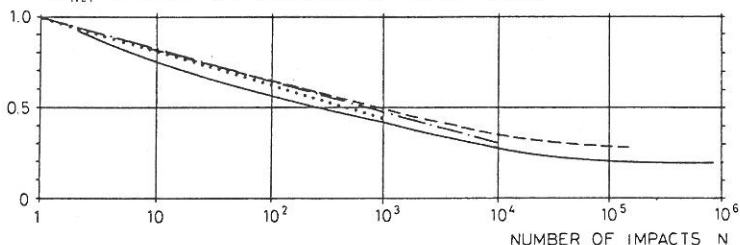
$$\frac{\Delta\sigma_N}{\Delta\sigma_{N=1}} = \frac{\text{ULTIMATE DYN. STRESS RANGE FOR } N \text{ IMPACTS}}{\text{ULTIMATE DYN. STRESS RANGE FOR ONE IMPACT}}$$


Fig. 12. Fatigue. Unreinforced concrete. Impact load.

It is seen that the graphs almost collapse into one single graph which then represents a universal curve for fatigue of *impact* loaded unreinforced concrete. Moreover, the graphs in Figs. 2 and 3 representing fatigue due to *pulsating* uniaxial loads fall into one graph. Because it seems most likely that also in this case fatigue due to pulsating flexural load follows this graph one can then produce two universal graphs as shown in Fig. 13, one representing fatigue by impact load and one representing pulsating load.

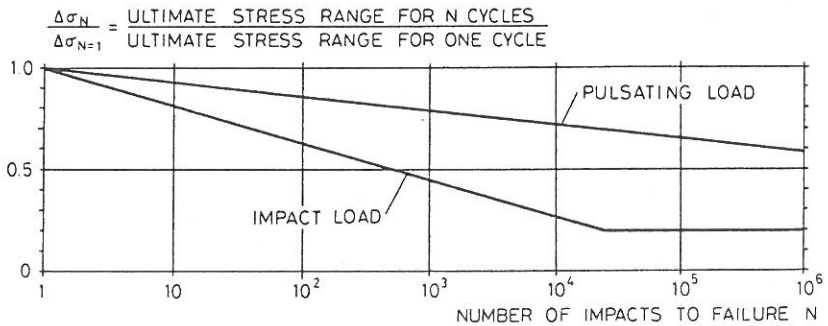


Fig. 13. Fatigue in conventional unreinforced concrete. Uniaxial and flexural stress.

Having in mind the uncertainties on the important parameters involved in rubble mound breakwater design, the graphs in Fig. 13 are regarded accurate enough for practical design of armour layers made of conventional unreinforced concrete blocks. It should be noted that the ultimate *impact* load strength for one cycle is in the order of 1.4 and 1.5 times the ultimate *pulsating* load strength in the case of uniaxial tension and compression respectively, cf. Fig. 2. For flexural stresses a factor of app. 1.4 should be used.

The ultimate pulsating load strength properties for one cycle can be taken equal to the static ones.

IMPLEMENTATION OF FATIGUE IN THE DESIGN PROCESS

The fatigue life is usually evaluated according to the *Palmgren-Minor accumulated damage theory* on the basis of a propoiate Wöhler diagram, e.g. Fig. 13.

The Palmgren-Minor rule expressing the cumulative damage ration, D reads

$$D = \sum_{i=1}^K \frac{\eta_i}{N_i} \leq 1, \quad (6)$$

where η_i is the number of cycles within the stress range interval i , N_i is the number of cycles to failure at the same stress range derived from the Wöhler diagram and K is the total num-

ber of stress range intervals. This implies that the number of stress cycles and the corresponding stress ranges throughout the lifetime of the structure, i.e. η , N and K in eq. (6), must be estimated. This again means that the *load history* and the *relationship between the load and the stresses* must be established.

Pure deterministic calculations are impossible. More realistic is a *stochastic* approach.

In breakwater engineering the load history is closely tied up with the wave history. In most places a reasonable estimate on the wave history can be obtained from hindcast studies or observations. The wave history may be presented as the variation in significant wave height, H_s with the time, t , see Fig. 14.

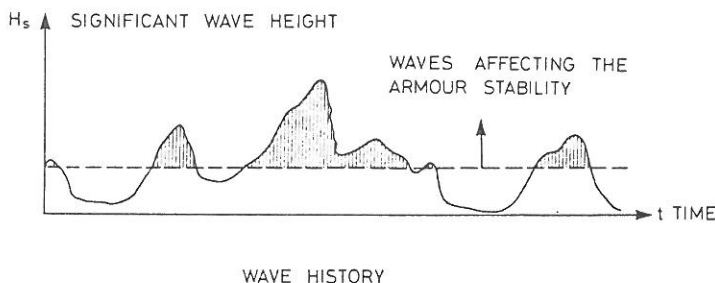


Fig. 14. Wave history.

The wave period which is also of great importance is included in this representation if a relationship between wave height and period is established; for example is a power relationship often found. Only waves or storms over a certain size will contribute to the stability conditions of the armour block. The cut-off level, shown as a dotted line in the figure, depends on many things of which the type, the size, the material strength properties and the location on the structure of the armour blocks are the most important. The cut-off level will be relatively low for complex types of units, especially for the big ones where the stresses are high due to their own weight alone. The cut-off level might vary with time due to change in the strength properties of the concrete or change in hydraulic stability, for example caused by abrasion of the blocks.

The storm history can be modelled as a weakly stationary, stochastic process with a specific intensity, and following a specific extreme distribution, for example a Weibull distribution. Further, if independence between storm event is assumed the starting times of the storms can be characterized by a Poisson counting process. The wave heights are Rayleigh distributed in intervals of stationarity.

The stresses in an armour unit can be split into three terms, cf. Fig. 1: The *static* stresses mainly due to gravity, the *pulsating* stresses due to flow forces generated by the waves and the *impact* stresses generated when units are rocking, displaced and hit by other units. The problem is to find the stress transfer functions i.e. the relationship between the stresses and the wave action on the specific location of the breakwater structure, as illustrated in Fig. 15.

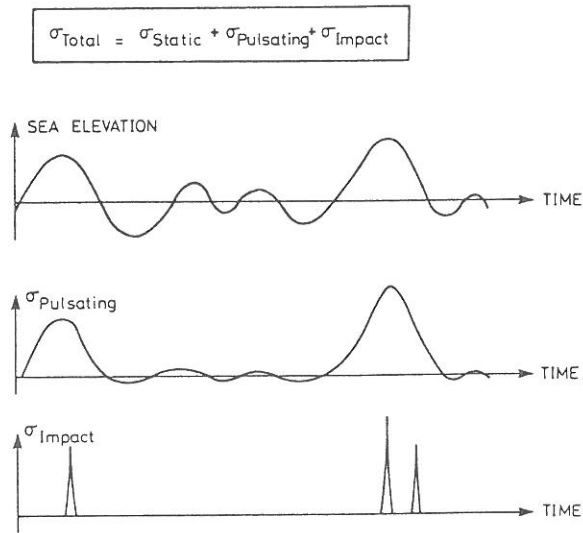


Fig. 15. Realization of wave induced stresses in an armour unit.

Due to the random placement of the armour units the stress transfer functions must be characterized by reference values (as for example the mean) and the distribution functions as illustrated on Fig. 16.

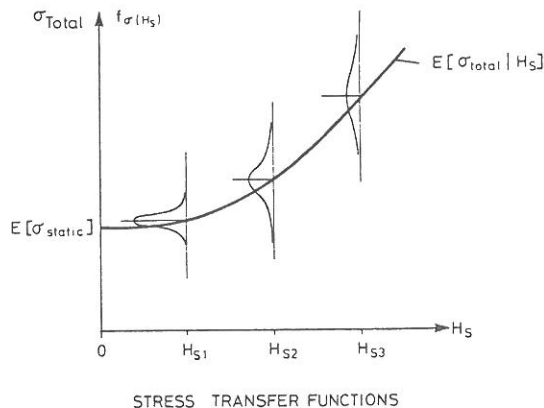


Fig. 16. Qualitative illustration of dependence of stress transfer frequency functions on wave parameter.

The static stress field might be established from strain gauge measurements on large scale model armour layers in the dry combined with similarity considerations.

The dynamic stress field is much more difficult to assess. Because prototype measurements are very difficult and expensive the problem must be studied in large scale hydraulic models mainly by strain gauge measurements. The huge amount of work necessary to meet the needs of the practical designer calls for international sponsorship and cooperation.

In a consistent design process the above discussed strength aspects must be linked to the hydraulic stability aspects. Ref. (12) titled "Stochastic design of rubble mound breakwaters" deals with this problem taking into account also impact fatigue based on an estimated simple stress transfer function.

ACKNOWLEDGEMENTS

The study was sponsored by The Danish Council for Scientific and Industrial Research. The cooperation of Mr. Sven Hvid Nielsen and Mr. J.Kr. Jehrbo Jensen, the help of Aalborg Portland Cement and Concrete Laboratory in preparing pilot tests with fibre reinforced beams and the discussions with Prof. D. Krajcinovic and Dr. A.J. Zielinski are gratefully acknowledged. N.B. Beton Aps and S.N. Simonsen & Co. are thanked for the supply of concrete and fibres.

REFERENCES

1. Burcharth, H.F.: Material, Structural Design of Armour Units. Proc. Seminar on Rubble Mound Breakwaters. Royal Inst. of Technology, Stockholm, Sweden. Bulletin No. TRITA-VBI-120, 1983.
2. Burcharth, H.F.: The Way Ahead. Proc. Conf. on Breakwaters — Design and Construction. Inst. of Civil Engineers, London, 1983.
3. Tepfers, R., Kutti, T.: Fatigue strength of plain ordinary and lightweight concrete. ACI-Journal, May 1979.
4. Tepfers, R.: Tensile fatigue strength of plain concrete. ACI-Journal, August 1979.
5. Fagerlund, G., Larsson, B.: Betongs slaghållfasthet (in Swedish). Swedish Cement and Concrete Research Institute at the Institute of Technology, Stockholm, 1979.
6. Zielinski, A.J., Reinhardt, H.W., Körmeling, H.A.: Experiments on concrete under repeated uniaxial impact tensile loading. RILEM Matériaux et Constructions, Vol. 14, No. 81, 1981.
7. Tait, R.B., Mills, R.D.W.B.: An investigation into the material limitations of breakwater Dolosse. ECOR newsletter No. 12, 1980.
8. Silva, M.G.A.: On the mechanical strength of cubic armour blocks. Proc. Coastal Structures '83, Washington, USA, 1983.
9. Burcharth, H.F.: Full scale trials of Dolosse to destruction. Proc. 17th Int. Conf. on Coastal Engineering, Sydney, 1980.
10. Burcharth, H.F.: Full scale dynamic testing of Dolosse to destruction. Coastal Engineering, 4, 1981.

11. Hippert, A.P., Hannant, D.J.: Impact resistance of fibre concrete. TRRL Supplementary Report 654. Transport and Road Research Laboratory, Dept. of the Environment. Berkshire, U.K.
12. Nielsen, S.R.K., Burcharth, H.F.: Stochastic design of rubble mound breakwaters. Laboratoriet for Hydraulik og Havnebygning, Aalborg University, June 1983. Short version: Proc. 11th IFIP Conf. on System Modelling and Optimization, Copenhagen 1983.